

General Disclaimer

One or more of the Following Statements may affect this Document

- This document has been reproduced from the best copy furnished by the organizational source. It is being released in the interest of making available as much information as possible.
- This document may contain data, which exceeds the sheet parameters. It was furnished in this condition by the organizational source and is the best copy available.
- This document may contain tone-on-tone or color graphs, charts and/or pictures, which have been reproduced in black and white.
- This document is paginated as submitted by the original source.
- Portions of this document are not fully legible due to the historical nature of some of the material. However, it is the best reproduction available from the original submission.

**NASA TECHNICAL
MEMORANDUM**

NASA TM X-74023

NASA TM X-74023

**(NASA-TM-X-74023) CALIBRATION OF A
UNIVERSAL INDICATED TURBULENCE SYSTEM (NASA)
37 p HC A03/HF A01 CSCL 14B**

N77-21400

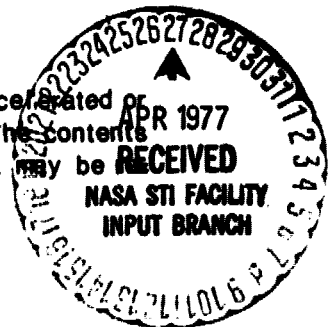
**G3/35 Unclas
24431**

**CALIBRATION OF A UNIVERSAL INDICATED
TURBULENCE SYSTEM**

William G. Chapin

March 1977

This informal documentation medium is used to provide accelerated or special release of technical information to selected users. The contents may not meet NASA formal editing and publication standards, may be revised, or may be incorporated in another publication.



**NATIONAL AERONAUTICS AND SPACE ADMINISTRATION
LANGLEY RESEARCH CENTER, HAMPTON, VIRGINIA 23665**

1. Report No. NASA TM X-74023		2. Government Accession No.		3. Recipient's Catalog No.	
4. Title and Subtitle Calibration of a Universal Indicated Turbulence System				5. Report Date March 8, 1977	
				6. Performing Organization Code 1277	
7. Author(s) William G. Chapin				8. Performing Organization Report No.	
9. Performing Organization Name and Address Langley Research Center Hampton, VA 23665				10. Work Unit No. 505-10-11-02	
				11. Contract or Grant No.	
12. Sponsoring Agency Name and Address National Aeronautics and Space Administration Washington, DC 20546				13. Type of Report and Period Covered Technical Memorandum	
				14. Sponsoring Agency Code	
15. Supplementary Notes					
16. Abstract <p>Theoretical and experimental work on a Universal Indicated Turbulence Meter is described. A mathematical transfer function from turbulence input to $\epsilon^{1/3}$ output indication was developed. A random ergodic process and a Gaussian turbulence distribution were assumed. A calibration technique based on this transfer function was developed. In order to properly adjust the system gain, it was necessary to experimentally determine the transfer function of the filter in the computer part of the system.</p> <p>The computer contains a variable gain amplifier to make the system output independent of average velocity. The range over which this independence holds was determined. An optimum dynamic response was obtained for the tubulation between the system pitot tube and pressure transducer by making dynamic response measurements for orifices of various lengths and diameters at the source end.</p> <p>Although no attempt was made to check all specifications, the tests performed showed that the Universal Indicated Turbulence Meter should perform satisfactorily.</p>					
17. Key Words (Suggested by Author(s)) Atmospheric turbulence measurement Universal indicated turbulence system Airplane ride quality			18. Distribution Statement Unclassified - Unlimited Star Category		
19. Security Classif. (of this report) Unclassified		20. Security Classif. (of this page) Unclassified		21. No. of Pages 35	
				22. Price* \$4.00	

CALIBRATION OF A UNIVERSAL INDICATED TURBULENCE SYSTEM

William G. Chapin
Langley Research Center

SUMMARY

Theoretical and experimental work on a Universal Indicated Turbulence Meter is described. A mathematical transfer function from turbulence input to $\epsilon^{1/3}$ output indication was developed. A random ergodic process and a Gaussian turbulence distribution were assumed. A calibration technique based on this transfer function was developed. In order to properly adjust the system gain, it was necessary to experimentally determine the transfer function of the filter in the computer part of the system.

The computer contains a variable gain amplifier to make the system output independent of average velocity. The range over which this independence holds was determined. An optimum dynamic response was obtained for the tubulation between the system pitot tube and pressure transducer by making dynamic response measurements for orifices of various lengths and diameters at the source end.

Although no attempt was made to check all specifications, the tests performed showed that the Universal Indicated Turbulence Meter should perform satisfactorily.

INTRODUCTION

This report describes the calibration and performance tests made on a Universal Indicated Turbulence System (UITS), model 1120, manufactured by Meteorology Research, Inc. Since no detailed information could be found either in the instruction manual (ref. 1) or elsewhere in the literature, a report on the work done would be a useful guide in calibrating and testing future systems.

The UITS is used by Langley Research Center's Flight Dynamics and Control engineers to measure atmospheric turbulence intensity in the inertial subrange as part of an airplane ride quality program. The inertial subrange of the turbulence extends from less than 1 Hz to about 1 kHz. It has been found that all sensations of turbulence experienced by aircraft passengers are due to transverse frequencies within the inertial subrange (ref. 2).

No mathematical expression describing the transfer function of the system from turbulence input to final output could be found in the literature;

therefore, the theoretical transfer function was derived assuming a Gaussian amplitude distribution and an ergodic process.

SYMBOLS

$A(f)$	frequency response characteristic of a general linear system
$B(f)$	frequency response characteristic of computer filter
$B(f_c)$	frequency response of filter at the calibration frequency
c	computer system constant equal to $c_v c_f c_r c_d$, where the individual constants are as shown in figure 3
c_2	universal dimensionless constant equal to about 0.15 (ref. 2)
D	output indicator deflection - $\epsilon^{1/3}$ units
f	frequency - Hz
f_c	calibration frequency - Hz
f_h	frequency definitely within inertial subrange above which the power spectral density of the filtered signal is negligible - Hz
f_l	frequency definitely within inertial subrange below which the power spectral density amplitudes of the filtered signal are negligible - Hz
$G(f)$	single sided power spectral density of a transverse component of turbulence in the inertial subrange
$h(t)$	time domain impulse response of the RC averaging circuit
$H(S)$	S domain transfer function of the RC averaging circuit

$$I_1 \quad \int_{f_l}^{f_h} |B(f)|^2 f^{-5/3} df$$

$$I_2 \quad \int_{f_l}^{f_h} \left| \frac{B(f)}{B(f_c)} \right|^2 f^{-5/3} df$$

K	system gain constant with meaning as implied in usage
$p(t)$	total differential pressure due to $u(t)$ - F/L^2
$p_d(t)$	dynamic component of differential pressure - F/L^2
p_o	static component of differential pressure - F/L^2
t	time
T	averaging time
$u(t)$	instantaneous total longitudinal velocity relative to a moving sensor - L/T
$u_d(t)$	dynamic component of the above velocity - L/T
u_o	average component of $u(t)$ - L/T
$U(f)$	single sided power spectral density of $u_d(t)$
$U_1(f)$	low frequency portion of $U(f)$ which has negligible amplitude at the output of the UITS filter. This includes a component due to inertial subrange turbulence and also deterministic components such as inputs from the pilot or autopilot.
$U_2(f)$	that part of the single sided power spectral density definitely within the inertial subrange
$U_3(f)$	that part of the single sided power spectral density containing those upper frequencies which when filtered out have negligible amplitudes. Some of these frequencies may be in the inertial subrange.
$U_{sr}(f)$	single sided power spectral density of the inertial subrange of $U(f)$. This includes all of $U_2(f)$ and parts of $U_1(f)$ and $U_3(f)$.
v_c	input ac calibration voltage
v_{cpp}	peak-to-peak input calibration voltage
v_{crms}	rms ac input calibration voltage
V_{3cpp}	peak-to-peak calibration voltage at the output of the filter
$v_i(t)$	instantaneous voltage output at various stages of the UITS computer; $i = 1, 2, 3, 4, 5$
$v_{id}(t)$	ac voltage outputs at various stages of the UITS computer

v_{io}	dc voltage components
v_{loc}	calibration dc bias voltage
v_o	dc output voltage of computer unit
$\frac{1}{x^2}$	mean square value of the dynamic component of an ergodic signal, $x_d(t)$, where $x_d = u_d, v_{id}$
$X(f)$	corresponding power spectral density of $x_d(t)$
ϵ	rate at which turbulent energy is converted into heat - L^2/T^3
$\theta(f)$	power spectral density of the output of a general linear system
ρ	density FT^2/L^4
ρ_o	density for which the system is calibrated
$\phi(f)$	power spectral density of the input of a general linear system

Subscript "fs" denotes full scale value of a variable. Capital letters denote the power spectral density associated with the dynamic component of a time domain variable, the system frequency response function, or the S domain function.

DESCRIPTION OF SYSTEM

A block diagram of the system is shown in figure 1 (ref. 1). It consists of a pitot tube, pressure transducer, a computer unit, and an output meter. The computer unit contains a variable gain amplifier, a constant gain ac amplifier, a filter, a half wave rectifier, an RC averaging circuit having a 3-second time constant, and a constant gain dc amplifier. The system, except for the pitot tube, is shown in figure 2.

The signal path is shown in figure 3. The pitot tube senses the differential pressure produced by the air velocity. The velocity signal consists of both steady state and turbulence components. As will be shown in the theoretical development, the system output, D , is made independent of the static velocity, u_o , by making the gain of the variable gain amplifier proportional to $v_{io}^{-2/3}$. The half wave rectifier and RC circuit averages the random signal output from the filter. The output of the computer unit is transmitted to the output indicator which is a dc voltmeter calibrated in $\epsilon^{1/3}$ units. Full scale on the indicator corresponds to 5 Vdc and an $\epsilon^{1/3}$ of $10 \text{ cm}^{2/3} \text{ sec}^{-1}$.

As will be shown in the theoretical development, the exact shape of the filter frequency response characteristic is unimportant, but greatest

system gain is obtained with the pass band of the filter at the lowest frequencies; however, a design compromise is necessary, since there is a need to eliminate very low frequencies outside the inertial subrange and 1 to 2 Hz inputs from the pilot or autopilot (ref. 3).

THEORY

Background Information

Kolmogoroff, in 1941, reasoned that there would be a portion of the turbulence spectrum that could be represented by one number, ϵ , the rate at which energy is converted into heat. This portion of the spectrum is called the inertial subrange (ref. 2). In the inertial subrange,

$$U_{sr}(f) = \frac{3}{4} G(f) = c_2 u_o^{2/3} \epsilon^{2/3} f^{-5/3} \quad (1)$$

It is uncertain as to what are the upper and lower limits of the inertial subrange. They are dependent on average velocity. Empirical data suggests, for example, that for a 45 m/sec (100 mph) airspeed, the inertial subrange extends from about 0.15 Hz to about 1 kHz (ref. 2). Due to the electronic filter in the UITS, exact knowledge of these limits is not necessary.

Development of UITS Transfer Function

The power spectral density of all the turbulence components can be written as $U(f)$. $U(f)$ can be written as

$$U(f) = U_1(f) + U_2(f) + U_3(f) \quad (2)$$

In equation (2) and in the rest of the mathematical development, it is assumed that zero frequency components due to mean values are not included in the power spectral density expressions.

$U_2(f)$ is assumed to be ergodic. That is, for any one burst of turbulence, the turbulence intensity is theoretically, after transient effects have died out, a constant proportional to $\epsilon^{1/3}$ after a long (theoretically infinite) averaging time. Then,

$$\int_{0^+}^{\infty} U(f) df = \int_{0^+}^{f_l} U_1(f) df + \int_{f_l}^{f_h} U_2(f) df + \int_{f_h}^{\infty} U_3(f) df. \quad (3)$$

The "o+" denotes the fact that the power spectral density component due to u_o is not included. Hereafter, it will be assumed that a zero integration limit does not include a mean value, and the + symbol will not be used.

$$p(t) = \frac{1}{2} \rho u^2(t) \quad (4a)$$

and

$$dp = \rho u du$$

For small $u_d(t)/u_o$, $dp \cong p_d(t)$; $du \cong u_d(t)$; and $u \cong u_o$.

Therefore

$$p_d(t) = \rho u_o u_d(t) \quad (4b)$$

In general (ref. 4), $\theta(f) = |A(f)|^2 \phi(f)$

If $|A(f)| = K$, a constant, then $\theta(f) = K^2 \phi(f)$.

Therefore,

$$P(f) = \rho^2 u_o^2 U(f) \quad (4c)$$

Similarly, as seen from figure 3,

$$V_1(f) = c_p^2 P(f) \quad (5a)$$

$$V_2(f) = c_v^2 v_{lo}^{-4/3} V_1(f) \quad (5b)$$

$$V_3(f) = c_f^2 |B(f)|^2 V_2(f) \quad (5c)$$

From equations (4c), (5a), (5b), and (5c), there is obtained

$$V_3(f) = c_p^2 c_v^2 c_f^2 v_{lo}^{-4/3} \rho^2 u_o^2 |B(f)|^2 U(f)$$

and

$$\int_0^{\infty} v_3(f) df = c_p^2 c_v^2 c_f^2 v_{10}^{-4/3} \rho^2 u_o^2 \int_0^{\infty} |B(f)|^2 U(f) df. \quad (6a)$$

Since $|B(f)|^2 U_1(f)$ and $|B(f)|^2 U_3(f)$ are assumed negligible, equation (6a) to a close approximation can be written as

$$\int_0^{\infty} v_3(f) df = c_p^2 c_v^2 c_f^2 v_{10}^{-4/3} \rho^2 u_o^2 \int_{f_l}^{f_h} |B(f)|^2 U_2(f) df \quad (6b)$$

Since in the frequency range covered by $U_2(f)$, $U_2(f) = U_{gr}(f)$, equation (1) can be substituted into equation (6b) with the result that

$$\int_0^{\infty} v_3(f) df = c_p^2 c_v^2 c_f^2 c_2 v_{10}^{-4/3} \rho^2 u_o^{8/3} \times \left[\int_{f_l}^{f_h} |B(f)|^2 f^{-5/3} df \right] \epsilon^{2/3} \quad (6c)$$

For an ergodic process (ref. 4),

$$\overline{x_d^2} = \lim_{T \rightarrow \infty} \frac{1}{T} \int_0^T x_d^2(t) dt = \int_0^{\infty} x(f) df$$

Therefore

$$\overline{v_{3d}^2} = \int_0^{\infty} v_3(f) df \quad (7)$$

Since $v_{3d}(t) = v_3(t)$, the "d" subscript will no longer be used.

From equations (7) and (6c),

$$\overline{v_3^2} = c_p^2 c_v^2 c_f^2 c_2 v_{10}^{-4/3} \rho^2 u_o^{8/3} I_1 \epsilon^{2/3} \quad (8)$$

The symbol I_1 has been used in place of the integral expression.

Next, the output of the system will be determined in terms of $\overline{v_3^2}$. If the assumption is made that $u_d(t)$ is Gaussian, it can be shown that $v_3(t)$ is Gaussian (ref. 4). For a zero mean value,

$$\overline{v_3^2} = \int_{-\infty}^{\infty} \frac{v_3^2 \exp\left(\frac{-v_3^2}{2\sigma^2}\right)}{\sigma(2\pi)^{1/2}} dv_3$$

When this integral is evaluated, it is found to equal σ^2 (ref. 4). Therefore,

$$\overline{v_3^2} = \sigma^2 \quad (9)$$

The average value of the output of the half wave rectifier is

$$\overline{v_4} = c_r \int_0^{\infty} \frac{v_3 \exp(-v_3^2/2\sigma^2)}{\sigma(2\pi)^{1/2}} dv_3$$

The lower limit is due to the rectification action.

By making the substitution $y = v_3^2$, the integral can be evaluated with the result that

$$\overline{v_4} = \frac{c_r \sigma}{(2\pi)^{1/2}} \quad (10)$$

From equations (9) and (10)

$$\overline{v_4} = \frac{c_r \sqrt{v_3^2}}{(2\pi)^{1/2}} \quad (11)$$

An analysis will now be made of the averaging action of the RC circuit for an ergodic signal input. The equivalent circuit of the UITS RC circuit is shown in figure 4. The output, $v_5(t)$, does not appear in figure 3, since the RC circuit and dc amplifier are shown as one block. The loading effect of the dc amplifier is assumed to be negligible.

By the convolution theorem (ref. 4),

$$v_5(t) = \int_0^t v_4(t - \tau) h(\tau) d\tau \quad (12)$$

First, $h(\tau)$ needs to be determined. By straightforward circuit analysis methods, $H(S)$ is found to be

$$H(S) = \frac{1/RC}{(S + \frac{2}{RC})} \quad (13a)$$

However,

$$h(\tau) = L^{-1} \{H(S)\}$$

or

$$h(\tau) = \frac{\exp(-\frac{2\tau}{RC})}{RC} \quad (13b)$$

Therefore, from equations (12) and (13b)

$$v_5(t) = \frac{1}{RC} \int_0^t \exp(-\frac{2\tau}{RC}) v_4(t - \tau) d\tau \quad (14)$$

The average value of $v_5(t)$, $\overline{v_5}$, is defined for an ergodic process to be

$$\overline{v_5} = \lim_{T \rightarrow \infty} \frac{1}{T} \int_0^T v_5(t) dt \quad (15)$$

If equations (14) and (15) are combined, then

$$\overline{v_5} = \lim_{T \rightarrow \infty} \frac{1}{T} \int_0^T \frac{1}{RC} \int_0^t \exp\left(\frac{-2\tau}{RC}\right) v_4(t - \tau) d\tau dt$$

If the order of integration is reversed, and the limits of integration are appropriately changed, then

$$\overline{v_5} = \lim_{T \rightarrow \infty} \frac{1}{RC} \int_0^T \lim_{T \rightarrow \infty} \frac{1}{T} \int_{\tau}^T \exp\left(\frac{-2\tau}{RC}\right) v_4(t - \tau) dt d\tau \quad (16)$$

For an ergodic process

$$\lim_{T \rightarrow \infty} \frac{1}{T} \int_{\tau}^T v_4(t - \tau) dt = \overline{v_4} \quad (17)$$

where $\overline{v_4}$ is independent of t for very large T . Consequently, from equations (16) and (17),

$$\overline{v_5} = \lim_{T \rightarrow \infty} \frac{\overline{v_4}}{RC} \int_0^T \exp\left(\frac{-2\tau}{RC}\right) d\tau$$

If the above integration and limit operations are carried out, $\overline{v_5}$ is found to be

$$\overline{v_5} = \frac{\overline{v_4}}{2}$$

The conclusion is that for an ergodic process, the average value of the output voltage of the RC circuit is directly proportional to the average value of the input voltage.

Based on this conclusion,

$$v_o = c_d \overline{v_4} \quad (18)$$

As seen in figure 3, the constant, c_d , takes into account both the RC averaging circuit and the dc amplifier. By combining equations (8), (11), and (18),

$$v_o = (2\pi)^{-1/2} c_p c c_2^{1/2} \rho v_{10}^{-2/3} u_o^{4/3} I_1^{1/2} \epsilon^{1/3} \quad (19)$$

where c is as defined in the list of symbols.

Next, equation (19) will be modified to show that with the gain of the variable gain amplifier equal to $v_{10}^{-2/3}$, v_o is independent of u_o . From figure 3, for small $u_d(t)/u_o$,

$$\begin{aligned} v_{10} &= c_p p_o \\ &= \frac{1}{2} c_p \rho u_o^2 \end{aligned}$$

Therefore,

$$v_{10}^{-2/3} = c_p^{-2/3} 2^{2/3} \rho^{-2/3} u_o^{-4/3} \quad (20)$$

If equation (20) is substituted into equation (19), there results

$$v_o = 2^{1/6} \pi^{-1/2} c c_p^{1/3} c_2^{1/2} \rho^{1/3} I_1^{1/2} \epsilon^{1/3} \quad (21)$$

From figure 3,

$$D = c_m v_o \quad (22a)$$

Actually, D is a scale deflection. If the scale of D is thought of as

being in $\epsilon^{1/3}$ units, then

$$c_m \cong \frac{\epsilon_{fs}^{1/3}}{v_{ofs}}$$

and

$$D \cong \frac{\epsilon_{fs}^{1/3}}{v_{ofs}} v_o \quad (22b)$$

If equation (22b) is combined with equation (21), there results

$$D \cong 2^{1/6} \pi^{-1/2} \left(\frac{\epsilon_{fs}^{1/3}}{v_{ofs}} \right) c_p^{1/3} c_2^{1/2} \rho^{1/3} I_1^{1/2} \epsilon^{1/3} \quad (23)$$

Equation (21) is the basic relationship between the computer output and $\epsilon^{1/3}$, an index of turbulence intensity in the inertial subrange. Equation (23) is the basic relationship between the output indicator deflection and $\epsilon^{1/3}$. Equations (21) and (23) show that the system gain depends on $I_1^{1/2}$ and not on the exact frequency response characteristic of the filter. However,

since I_1 equals $\int_{f_l}^{f_h} |B(f)|^2 f^{-5/3} df$, it is desirable to pass as much of the low frequency portion of the inertial subrange spectrum as is possible.

Equations will now be developed which form the basis for the technique used to calibrate the UITS computer. A method is desired for adjusting the constant, c , so that the full-scale output indication, D_{fs} , corresponds to a desired $\epsilon_{fs}^{1/3}$. As seen from equation (23) the output depends on the density, ρ , and the sensitivity of the pressure transducer, c_p . Different desired operating conditions may require different transducer span adjustments. Essentially, the calibration technique is as follows: As shown in figure 5, a dc bias voltage, v_{loc} , is applied to the input of the computer to simulate the dc voltage from the pressure transducer. A sinusoidal voltage at a frequency, f_c , is applied in series with the bias voltage.

The peak-to-peak voltage, v_{3cpp} , at the output of the filter due to the input voltage, v_{cpp} , is

$$v_{3cpp} = c_v c_f |B(f_c)| v_{loc}^{-2/3} v_{cpp} \quad (24)$$

With half wave rectification and RC filtering, the dc output, v_o , of the system is

$$v_o = c_r c_d \frac{v_{3cpp}}{2\pi} \quad (25a)$$

From equations (22b) and (25a)

$$D \cong \frac{c_r c_d}{2\pi} \left(\frac{\epsilon_{fs}^{1/3}}{v_{ofs}} \right) v_{3cpp} \quad (25b)$$

If equation (24) is substituted into equation (25b), there results

$$D \cong \left(\frac{\epsilon_{fs}^{1/3}}{v_{ofs}} \right) \frac{c}{2\pi} |B(f_c)| v_{loc}^{-2/3} v_{cpp} \quad (25c)$$

If v_{cpp} is adjusted so that full scale output indication is obtained, equation (25c) can be equated to equation (23) with D and $\epsilon^{1/3}$ equal to their full scale values. The resulting equation can then be solved for v_{cpp} with the result that

$$v_{cpp} = 2^{7/6} \pi^{1/2} c_p^{1/3} c_2^{1/2} \rho^{1/3} v_{loc}^{2/3} \times \left[\int_{f_l}^{f_h} \left| \frac{B(f)}{B(f_c)} \right|^2 f^{-5/3} df \right]^{1/2} \epsilon_{fs}^{1/3} \quad (26a)$$

Equation (26a) can be expressed in an alternative manner since,

$$c_p = \frac{v_{lofs}}{p_{ofs}} \quad (26b)$$

If equation (26b) is substituted into equation (26a) and the symbol, I_2 , is used for the integral expression,

$$v_{cpp} = 2^{7/6} \pi^{1/2} \left(\frac{v_{lofs}}{p_{ofs}} \right)^{1/3} c_2^{1/2} \rho^{1/3} v_{loc}^{2/3} I_2^{1/2} \epsilon_{fs}^{1/3} \quad (26c)$$

From equations (26a) or (26c), then, the sinusoidal input voltage corresponding to $\epsilon_{fs}^{1/3}$ can be computed. The gain constant, c , is adjusted such that full scale output indicator deflection is obtained, or, for greater accuracy, such that the full-scale output voltage of the computer as measured with a precision dc voltmeter is obtained.

Next, the effect of atmospheric density, ρ , on the output indication will be shown. Suppose the tests were run at the same density as that at which V_{cpp} was computed. Then from a modification of equation (21) with $v_o = v_{ofs}$ and $\epsilon^{1/3} = \epsilon_{fs}^{1/3}$

$$\frac{\epsilon_{fs}^{1/3}}{v_{ofs}} = \left[2^{1/6} \pi^{-1/2} c_c^{1/3} c_2^{1/2} \rho^{1/3} I_1^{1/2} \right]^{-1} \quad (27)$$

If equation (27) is substituted into equation (23), there results

$$D \cong \epsilon^{1/3} \quad (28)$$

which is to be expected.

Suppose, however, that the system was adjusted on the basis of a calibration voltage calculated at a density of ρ_o but measurements are actually made at a density of ρ . If equation (27) with $\rho = \rho_o$, this time, is substituted into equation (21), there results:

$$D \cong \left(\frac{\rho}{\rho_o} \epsilon \right)^{1/3} \quad (29a)$$

or

$$\epsilon^{1/3} \cong \left(\frac{\rho_o}{\rho} \right)^{1/3} D \quad (29b)$$

That is, the apparent $\epsilon^{1/3}$ output, D , is multiplied by $\left(\frac{\rho_o}{\rho} \right)^{1/3}$ to get the true $\epsilon^{1/3}$.

TESTS

This section describes tests that were performed on the UITS. Although specifications were given in the instruction manual, no attempt has been made to check all specifications.

Figure 6 shows the experimental setup used for the tests on the computer. Dc power supply no. 1 furnished 28 Vdc power for the computer. Dc power supply no. 2 furnished a dc voltage bias to simulate the dc component of the output of the pressure transducer. The sinusoidal generator provided a sinusoidal signal needed for various tests. The dc voltmeter measured the output voltage of the system. The ac-dc voltmeter at the system input does not accurately measure ac voltages in the low millivolts range. Therefore, the signal was measured at a higher voltage level, and the voltage divider was used to apply a known portion of the measured signal to the input of the computer. The series combination of the bias voltage and the attenuated sinusoidal voltage was applied where the signal from the pressure transducer is normally applied.

The details are given in the instruction manual for adjusting the computer gain constant. A formula is given in the instruction manual for calculating the sinusoidal signal to be used in adjusting the gain of the computer.

It is: $v_{cpp} = \frac{64}{(p_{ofs})^{1/3}}$, where v_{cpp} is in mvpp and p_{ofs} is in psid. The

frequency of the sinusoidal signal is 12 Hz and the dc bias voltage is 2.5 Vdc. The "64" should be considered a nominal value. One of the purposes of the tests, of course, was to determine a more exact formula for the particular UITS being used.

Prior to the first test, the UITS computer was adjusted for a full scale output of 5 Vdc for a full scale pressure of $4.8 \times 10^3 \text{ N/m}^2$ (0.7 psid). At 15°C (59°F) and atmospheric pressure, this corresponds to an air speed of 89 m/sec (199 mph). v_{cpp} was found to be 72.1 mVpp or $v_{crms} = 25.5 \text{ mVrms}$. The pressure transducer had been previously calibrated and found to be linear.

A description follows of the tests performed.

Determination of I_2

As seen in equations (26a) or (26c), the value of this integral needs to be known in order to determine the desired sinusoidal calibration voltage.

The system output voltage was measured over the range from 1 Hz to 60 Hz with the input voltage at approximately 25.5 mVrms. As previously stated, this was the voltage that resulted in a full scale output of 5 Vdc at 12 Hz input frequency, which is f_c . The exact value of the input voltage was

recorded at each data point and used in the subsequent calculations. A small residual dc output voltage at zero input was subtracted from the measured dc output voltage. The resulting value of the output voltage shown differs from the ac output at the filter by a constant, which cancels out in calculating $\left| \frac{B(f)}{B(f_c)} \right|^2$. Outside of the above frequency limits, no system output could be detected.

Next, $\sum_{f=1}^{60} \left| \frac{B(f)}{B(f_c)} \right|^2 f^{-5/3} \Delta f$ was determined. From 1 to 5 Hz, Δf was 1 Hz. From 5 to 20 Hz, Δf was 0.5 Hz. From 20 Hz to 50 Hz, it was 1 Hz, and from 50 to 60 Hz, it was 2 Hz.

FDCD researchers decided to readjust the full scale voltage output of the pressure transducer so that it occurred at a pressure of $2.4 \times 10^3 \text{ N/m}^2$ (0.35 psid). This enabled the UITS to be used at a lower air speed. The pressure transducer was recalibrated and found to be linear. The gain of the UITS computer was correspondingly readjusted to make the full scale output voltage 5 Vdc. V_{cpp} was found to be 90.8 mVpp or 32.1 mV_{rms}.

The approximation to the integral was then determined for these conditions. It was also determined for output voltages at 12 Hz input of 4 V, 3 V, 2 V, and 1 V dc. For the 2 V case, the value of the summation was $0.230 \text{ Hz}^{-2/3}$. For all other cases, it was $0.229 \text{ Hz}^{-2/3}$.

Figure 7 shows the filter characteristic obtained for 5 Vdc full scale output at 12 Hz. There was no detectable difference in the characteristics obtained at other output voltages.

The calculation to establish the more exact formula for computing the calibration voltage follows. The density, ρ , is that at the standard temperature of 150C (590F)

$$v_{cpp} = \frac{2^{7/6} \pi^{1/2} v_{lofs}^{1/3} c_2^{1/2} \rho^{1/3} v_{loc}^{2/3} I_2^{1/2} \epsilon_{fs}^{1/3}}{p_{ofs}^{1/3}}$$

v_{cpp} is in Vpp. The result is to be stated in terms of $K/(p_{ofs})^{1/3}$ with p_{ofs} in psid.

$$v_{lofs} = 5 \text{ Vdc}$$

$$c_2 = 0.15$$

$$v_{loc} = 2.5 \text{ Vdc}$$

$$\rho = 1.23 \text{ kg/m}^3 (1.147 \times 10^{-7} \text{ lb-sec}^2/\text{in.}^4) \text{ (ref. 5)}$$

$$I_2 = 0.229 \text{ Hz}^{-2/3}$$

$$e_{fs}^{1/3} = 10 \text{ cm}^{2/3}/\text{sec} (5.37 \text{ in.}^{2/3}/\text{sec})$$

For the values listed, v_{cpp} was found to be

$$v_{cpp} = \frac{0.0606}{p_{ofs}^{1/3}} \quad v_{pp} = \frac{60.6}{p_{ofs}^{1/3}} \text{ mVpp}$$

Linearity Tests on the Computer

Amplitude linearity tests were made on the computer for bias voltages of 0.1, 0.6, 1.2, 2.5, and 5 Vdc. Results are shown in figures 8, 9, 10, 11, and 12.

Variable Gain Amplifier Tests

The UITS is usable only where v_{lo} is such that the gain of the variable gain amplifier varies as the $-2/3$ power. From equations (24) and (25a), with the input voltage expressed as rms rather than pp, the output voltage of the computer can be expressed as:

$$v_o = K v_{loc}^{-2/3} v_{crms}$$

or

$$\frac{v_{crms}}{v_o} = \frac{v_{loc}^{2/3}}{K}$$

The bias voltage, v_{loc} , was varied and v_{crms} was adjusted until v_o was about 5 Vdc. It was difficult to get v_o to exactly equal 5 Vdc, so the ratio v_{crms}/v_o was plotted against $v_{loc}^{2/3}$. This is shown in figure 13. It is to be noted that the desired gain is proportional to the inverse of $v_{loc}^{2/3}$. The voltage, v_{loc} , simulated the output of the pressure transducer.

The UITS is usable where v_{lo} is such that the curve is linear. This corresponds to $v_{lo}^{2/3} = 1.0 \text{ Vdc}^{2/3}$ or $v_{lo} = 1.0 \text{ Vdc}$. For a p_{ofs} of $2.4 \times 10^3 \text{ N/m}^2$ (0.35 psid) at a v_{lofs} of 5 Vdc, atmospheric pressure and 15°C (59°F), this corresponds to a u_o of 28 m/sec (63 mph).

Determination of Optimum Orifice Size for Pressure Tubulation System

For accurate measurements, it is necessary for the dynamic response of the tubing between the pitot tube and the pressure transducer to be as flat as possible. For a given tubing configuration, the response can be controlled to some extent by varying the diameter and length of an orifice placed at the source end of the tube.

A mock-up was made of the tubing configuration actually used on the airplane on which the UITs is to be used. This is shown in figure 14. A Bolt, Beranek, and Newman Model 901 D microphone calibrator was used as the source of dynamic pressure. A Pace CP-5 1DT $6.9 \times 10^2 \text{ N/m}^2$ (0.1 psid) pressure transducer was used as a reference transducer to measure pressure at the source end. Because of the physical size of the reference transducer and details of the calibrator not illustrated in figure 14, the source end of the tubing and the reference transducer could not be mounted flush with the dynamic pressure source. Dynamic response measurements were made for several different orifices. The results are shown in figure 15. The orifice number corresponds to the size of the drill used to drill the hole. No. 67 orifice (0.081 cm D, 1.27 cm L) is flat over the frequency range of most importance. It was decided to use this orifice for the next tests to be made with the UITs. The dynamic pressures applied at the source end varied in a given run with frequency and were between approximately 48.2 and 68.9 N/m^2 rms (7×10^{-3} and 10×10^{-3} psi rms).

Previous to the tests, the dynamic response of the tubulation between the "T" and the reference transducer was calculated using equations (6.89) and (6.90) on page 401 of reference 6. These equations are based on a second order constant coefficient differential equation model. The damping coefficient was found to be 0.02 and the natural frequency about 750 Hz. Therefore, the response can be considered essentially flat from 0 to 60 Hz.

CONCLUDING REMARKS

A mathematical transfer function from turbulence input to $\epsilon^{1/3}$ output indicator was derived for a Universal Indicated Turbulence System. From this, a calibration procedure was developed. Calibration and performance tests were made on a particular Universal Indicated Turbulence System, Model 1120, manufactured by Meteorology Research, Incorporated. The calibration procedure essentially consisted of inserting a 12 Hz sinusoidal signal at the input of the system computer and adjusting the computer gain for full scale $\epsilon^{1/3}$ output. In order to calculate the proper magnitude of this sinusoidal voltage, it was necessary to determine experimentally the transfer function of the computer filter. Within the operating range of the system, this transfer function was found to be amplitude invariant. Linearity tests on the computer at frequencies of 6, 12, and 20 Hz showed the computer characteristic to be linear.

Tests on the computer variable gain amplifier showed that the gain varied as the $-2/3$ power for dc input voltages above 1.0 Vdc. This $-2/3$ power variation is necessary for the proper operation of the system. At a density corresponding to 15°C (59°F), atmospheric pressure, and a full scale pressure transducer output voltage of 5 Vdc at $2.4 \times 10^3 \text{ N/m}^2$ (0.35 psid), the system is usable at a minimum airspeed of 28 m/sec (63 mph).

Tests were made to obtain the optimum dynamic response for the pressure tubing between the pitot tube and the pressure transducer. The response could be controlled to some extent by varying the diameter and length of an orifice placed at the source end of the tube. It was found that a #67 orifice (0.081 cm diameter, 1.27 cm length) gave the optimum response.

In conclusion, although no attempt was made to check all specifications, the tests that were performed showed that the instrument should perform satisfactorily.

REFERENCES

1. Meteorology Research, Inc.: Instruction Manual Universal Indicated Turbulence System Model 1120.
2. MacCready, Paul B., Jr.: Standardization of Gustiness Values from Aircraft, Journal of Applied Meteorology, Vol. 3, Aug. 1964, pp. 439-449.
3. MacCready, Paul B., Jr.; Williamson, Robin E.; Berman, Stephen; and Webster, Alexander: Operational Application of a Universal Turbulence Measuring System. NASA CR-62025, 1965.
4. Bendat, Julius S. and Piersol, Allan G.: Random Data: Analysis and Measurement Procedures, John Wiley and Sons, Inc., 1971.
5. Eshbach, Ovid W.: Handbook of Engineering Fundamentals, 2nd edition, John Wiley and Sons, Inc., 1952.
6. Doebelin, Ernest O.: Measurement Systems: Application and Design, McGraw Hill Book Company, 1966.

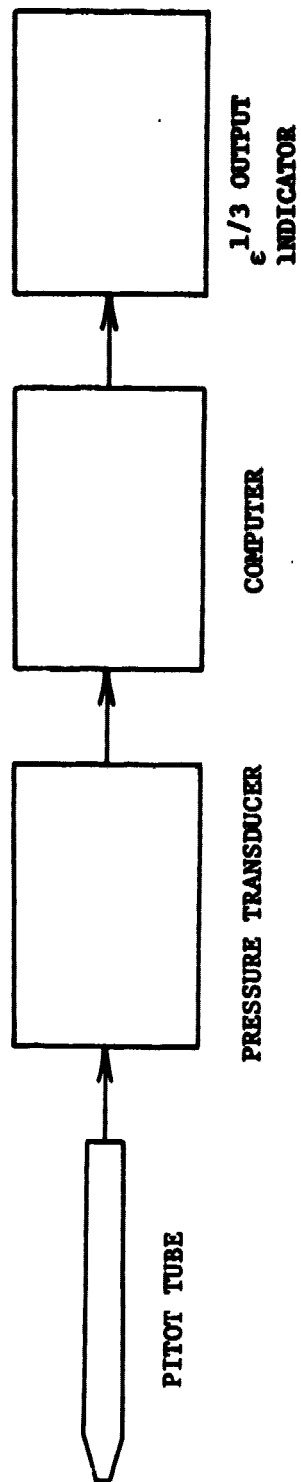


FIG. 1 - UNIVERSAL INDICATED TURBULENCE SYSTEM BLOCK DIAGRAM

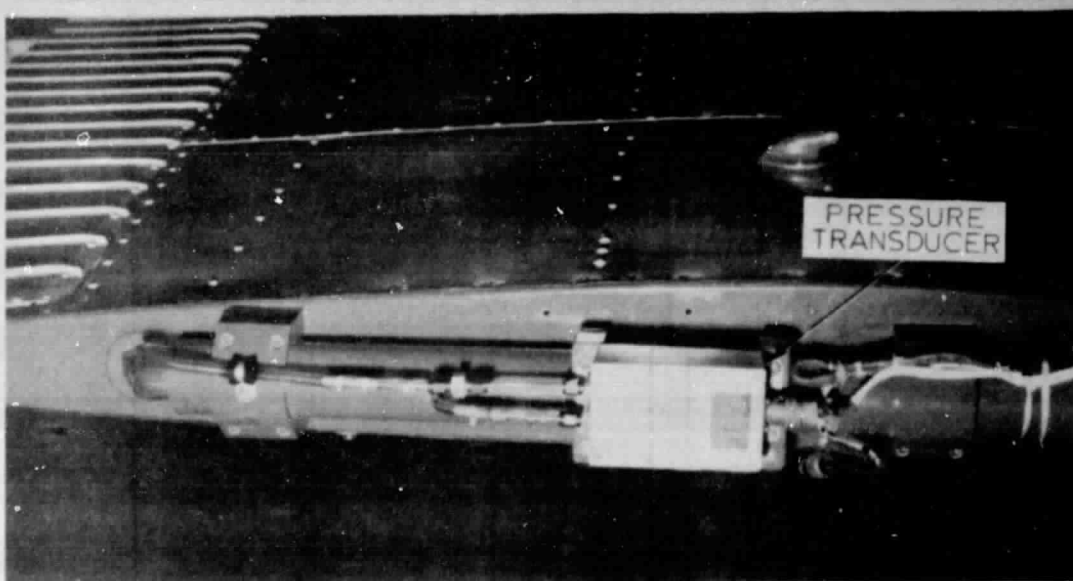
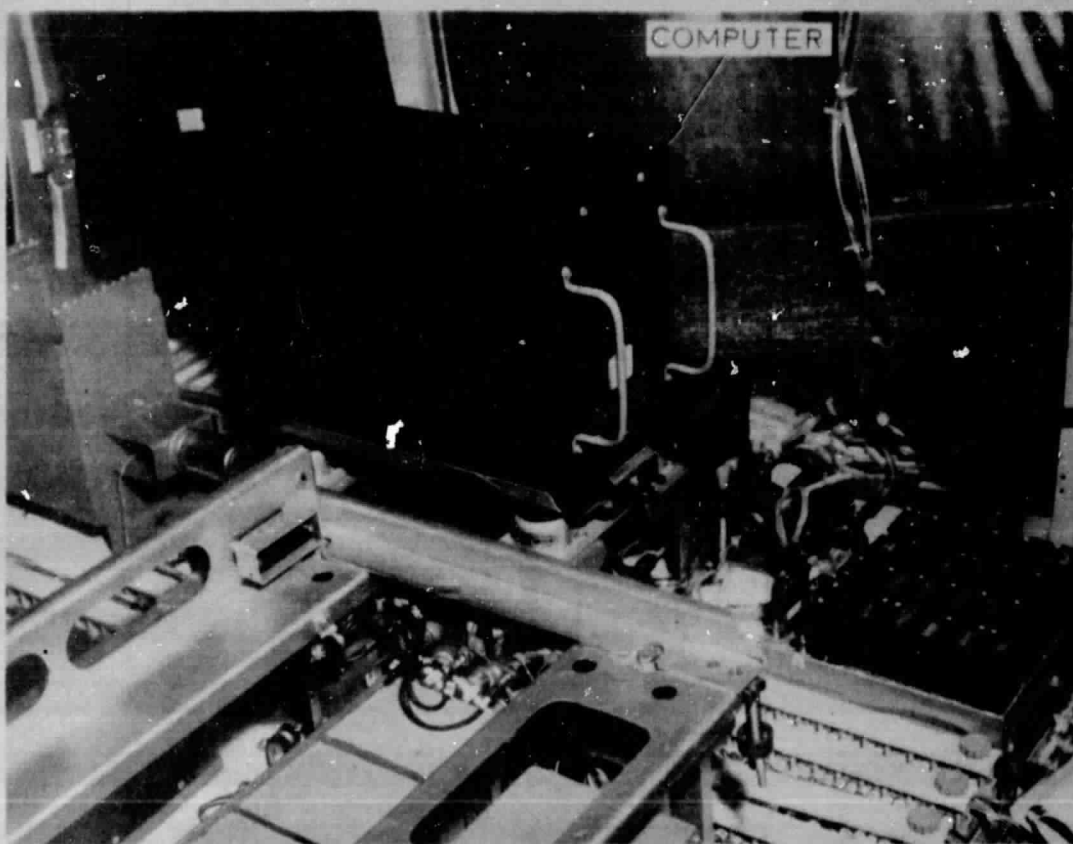


FIG. 2 UNIVERSAL INDICATED TURBULENCE SYSTEM

REPRODUCIBILITY OF THE
ORIGINAL PAGE IS POOR

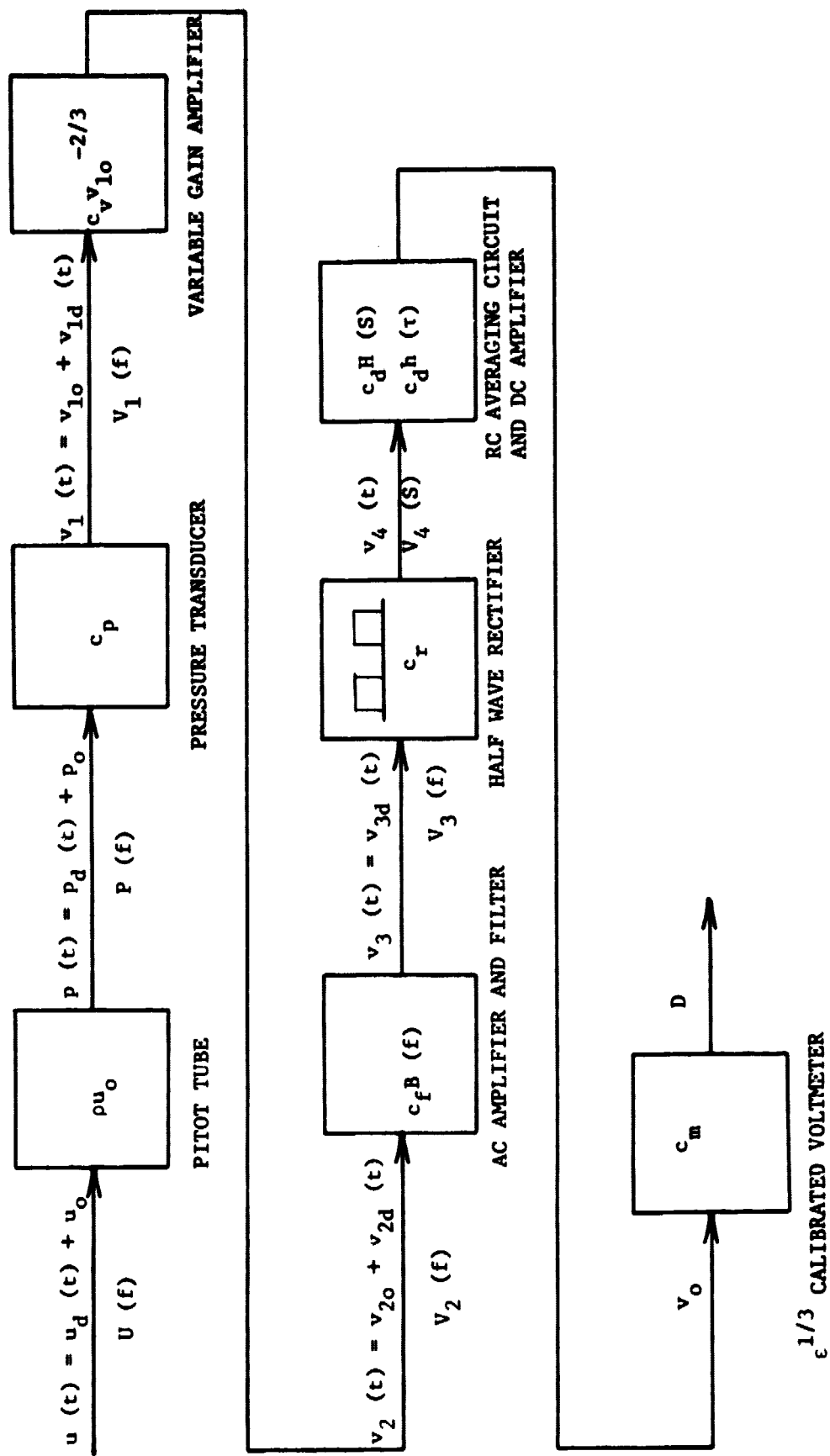


FIG. 3. DETAILED BLOCK DIAGRAM USED IN DETERMINATION OF TRANSFER FUNCTION

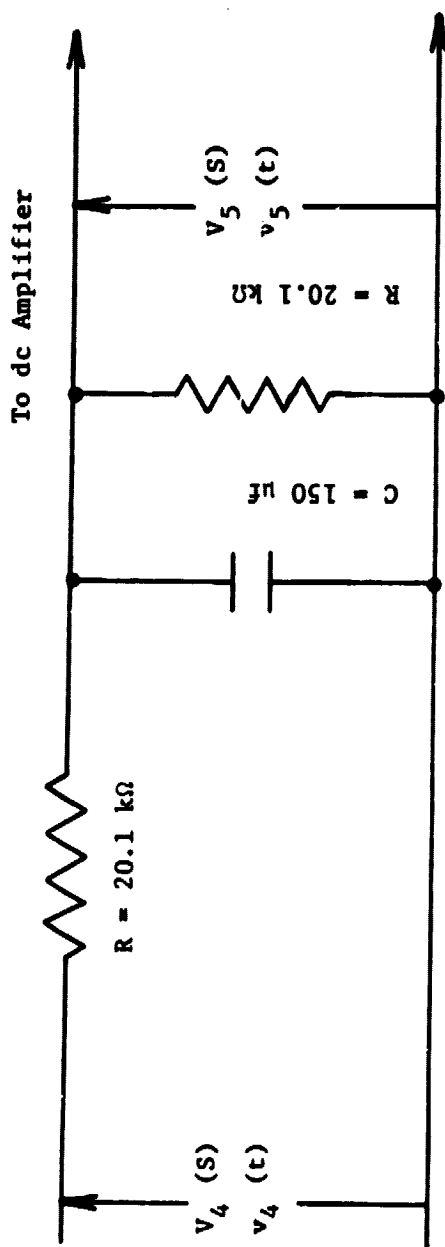


FIG. 4. EQUIVALENT RC AVERAGING CIRCUIT

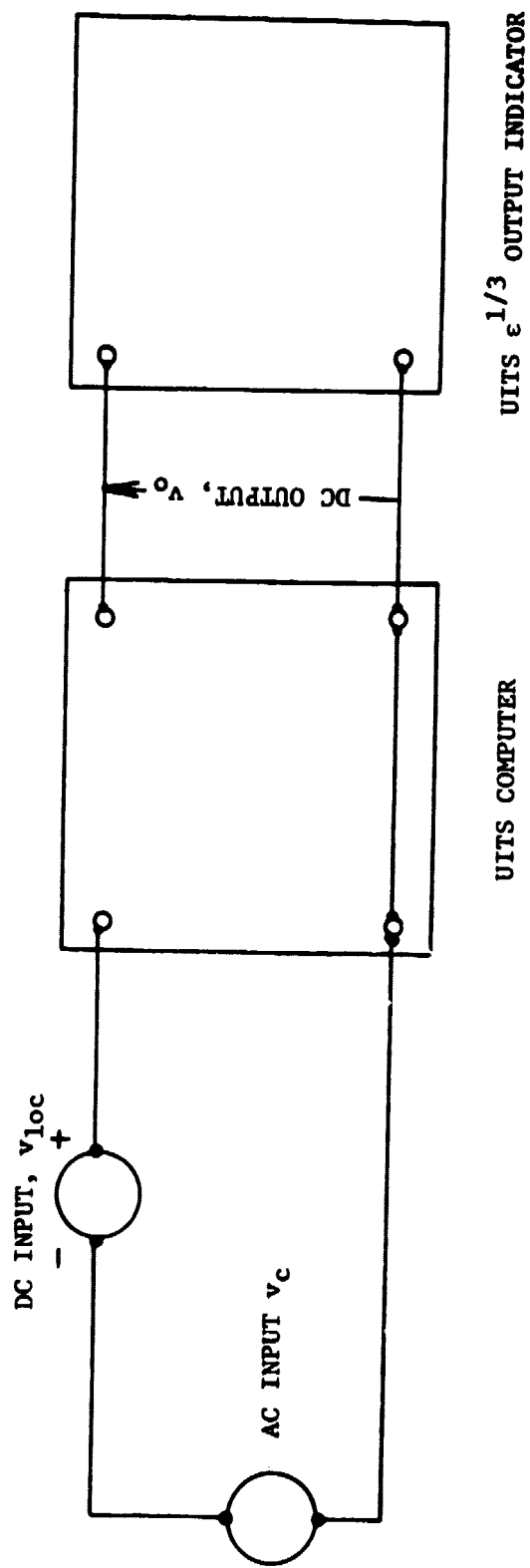


FIG. 5 - SIMPLIFIED DIAGRAM OF EXPERIMENTAL SETUP FOR TESTING THE UNIVERSAL INDICATED TURBULENCE SYSTEM COMPUTER

REPRODUCIBILITY OF THE
ORIGINAL PAGE IS POOR

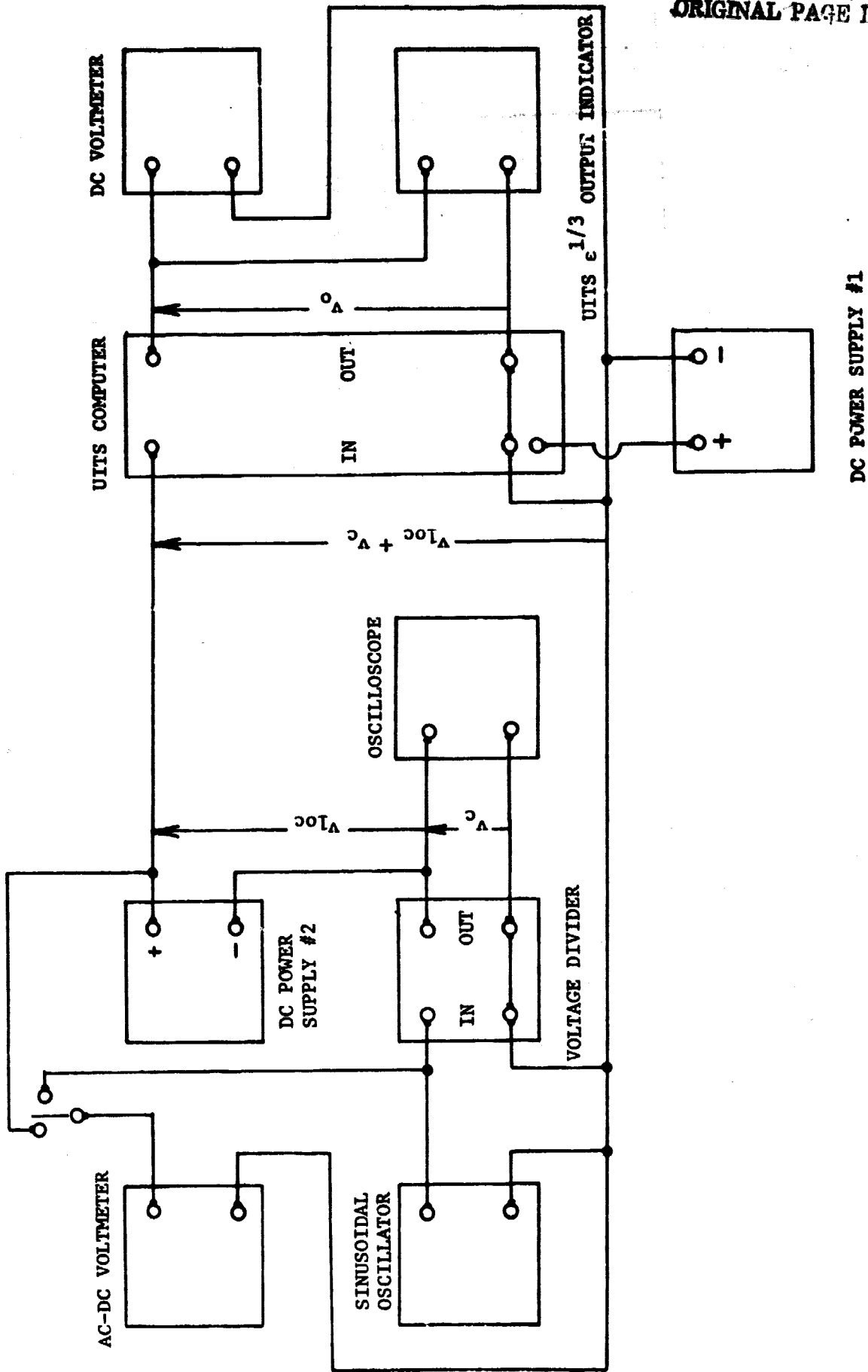


FIG. 6 - DIAGRAM OF EXPERIMENTAL SETUP FOR TESTING THE UNIVERSAL INDICATED TURBULENCE SYSTEM COMPUTER

Bias Voltage, v_{loc} : 2.5 v dc

Input Voltage, v_{crms} : 32.1 mVrms

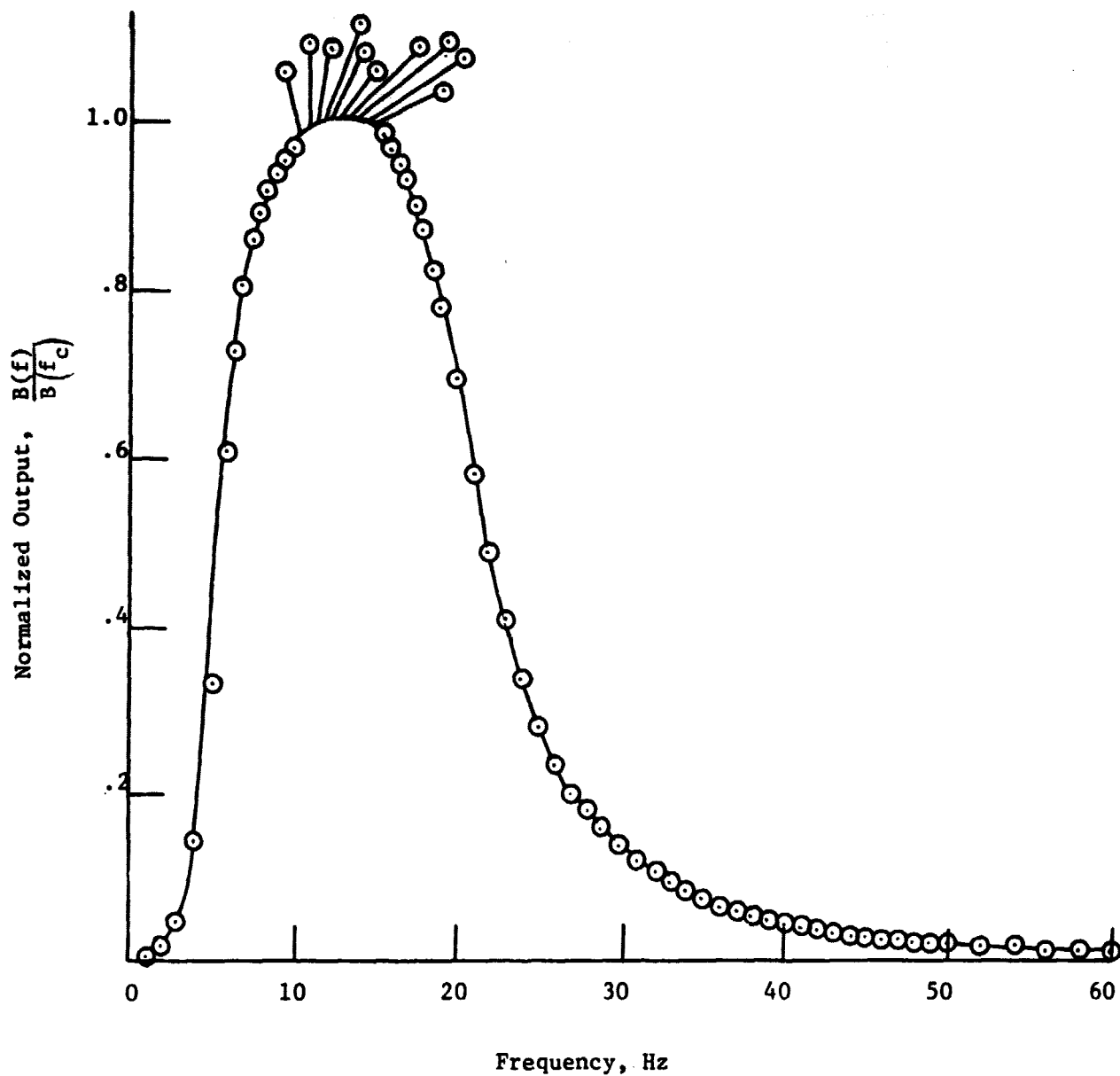


FIG. 7. UNIVERSAL INDICATED TURBULENCE SYSTEM FREQUENCY RESPONSE

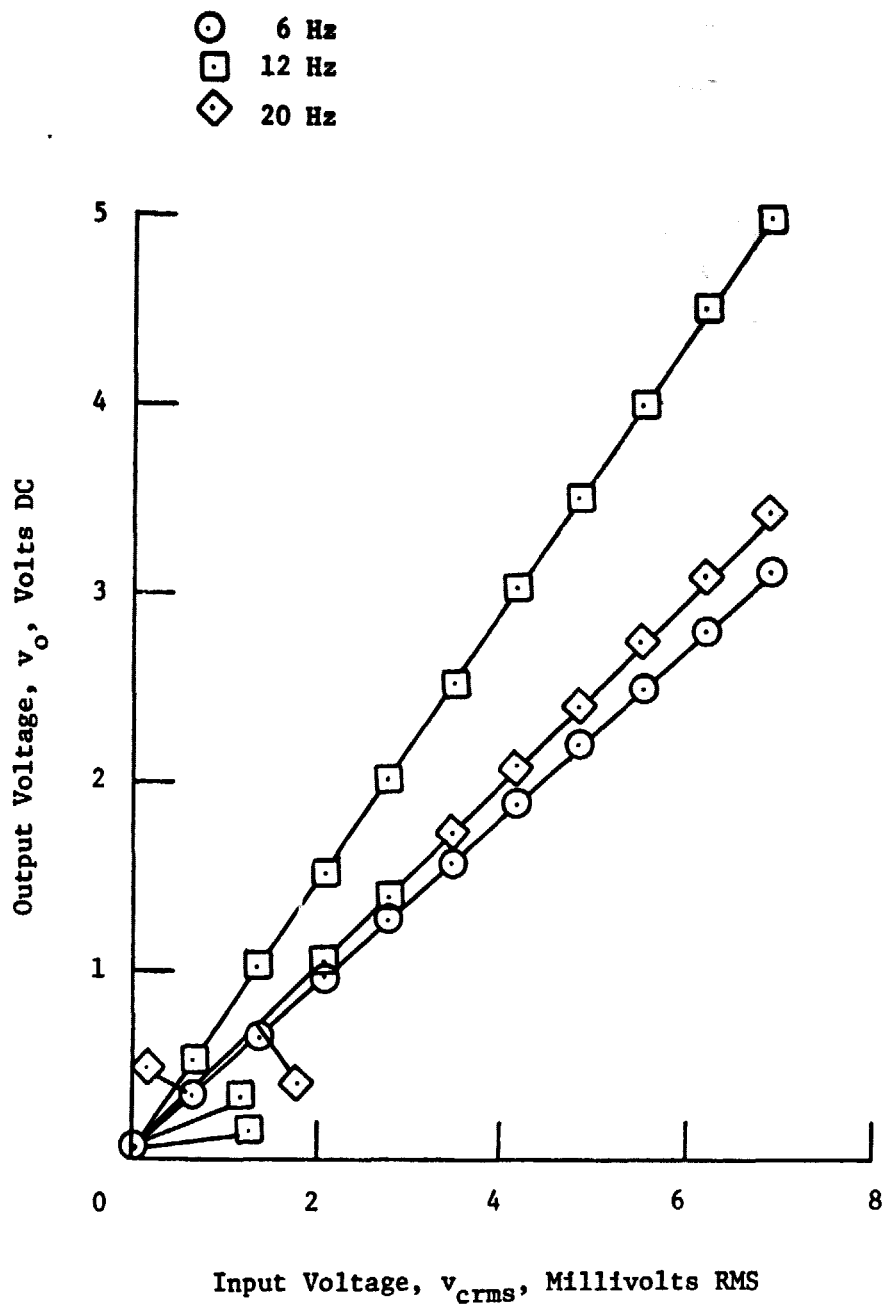


FIG. 8 - OUTPUT VOLTAGE VS. INPUT VOLTAGE FOR 0.1V DC BIAS VOLTAGE

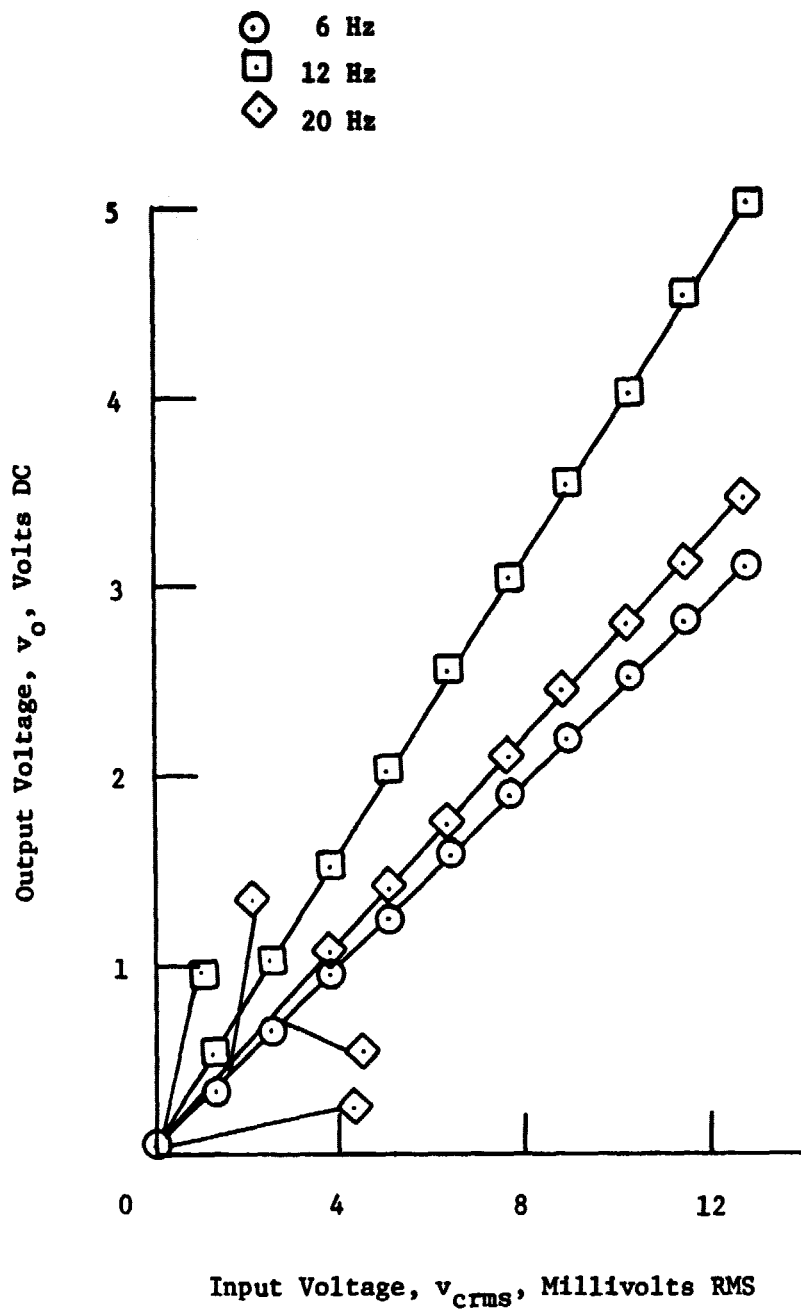


FIG. 9 - OUTPUT VOLTAGE VS. INPUT VOLTAGE FOR 0.6V DC BIAS VOLTAGE

- 6 Hz
- 12 Hz
- ◇ 20 Hz

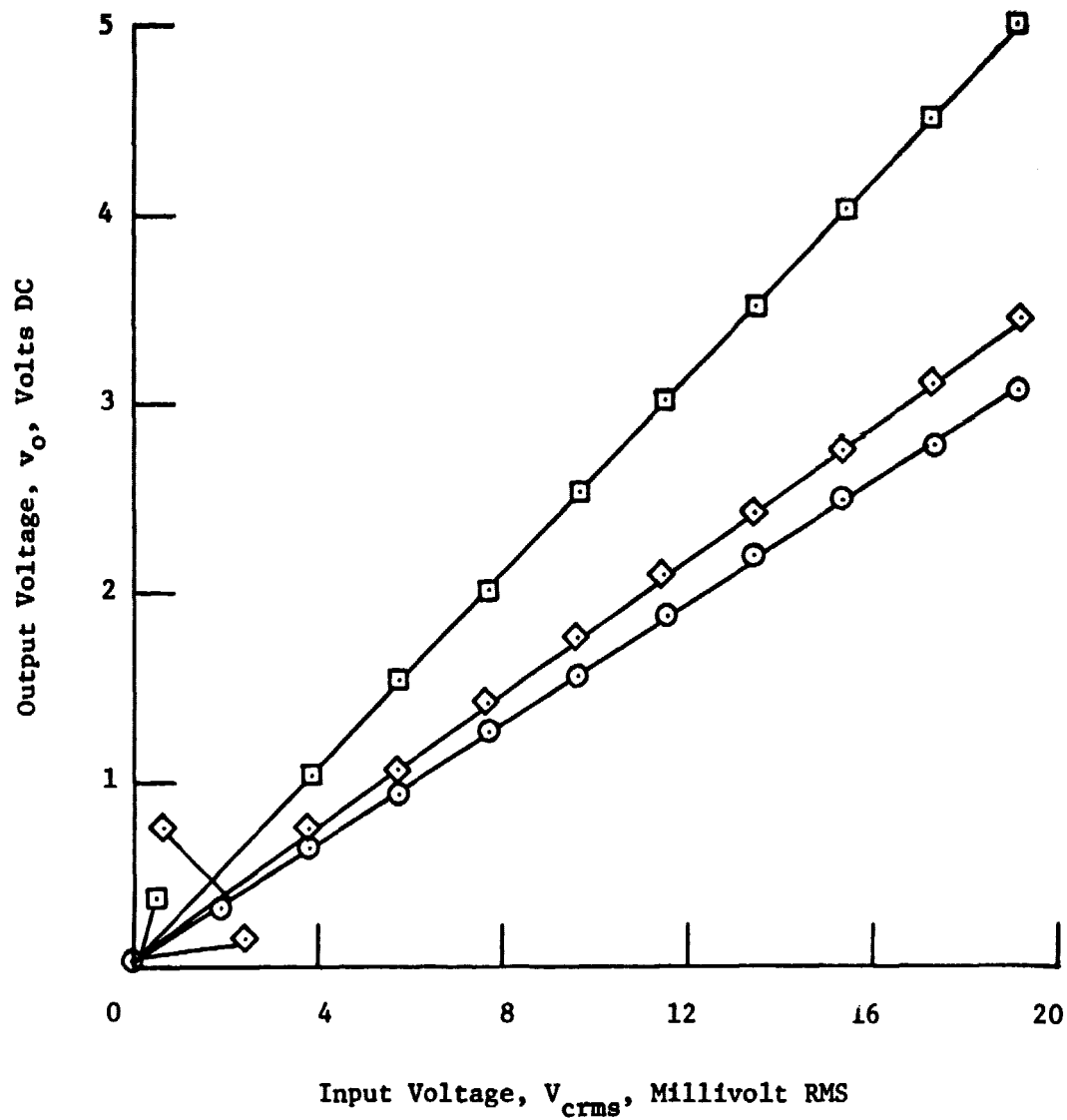


FIG. 10 - OUTPUT VOLTAGE VS. INPUT VOLTAGE FOR 1.2V DC BIAS VOLTAGE

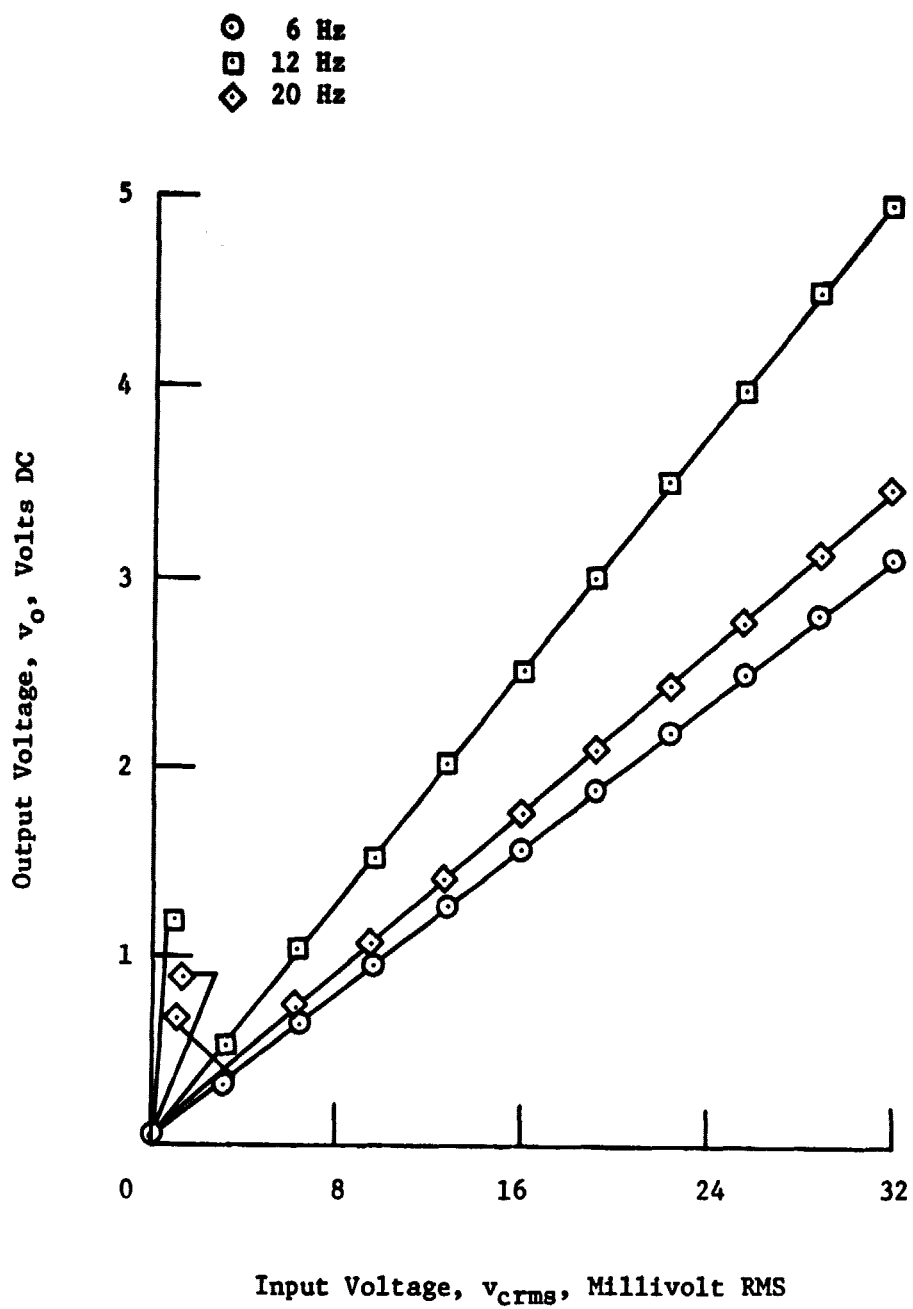


FIG. 11 - OUTPUT VOLTAGE VS. INPUT VOLTAGE FOR 2.5V DC BIAS VOLTAGE

- 6 Hz
- 12 Hz
- ◇ 20 Hz

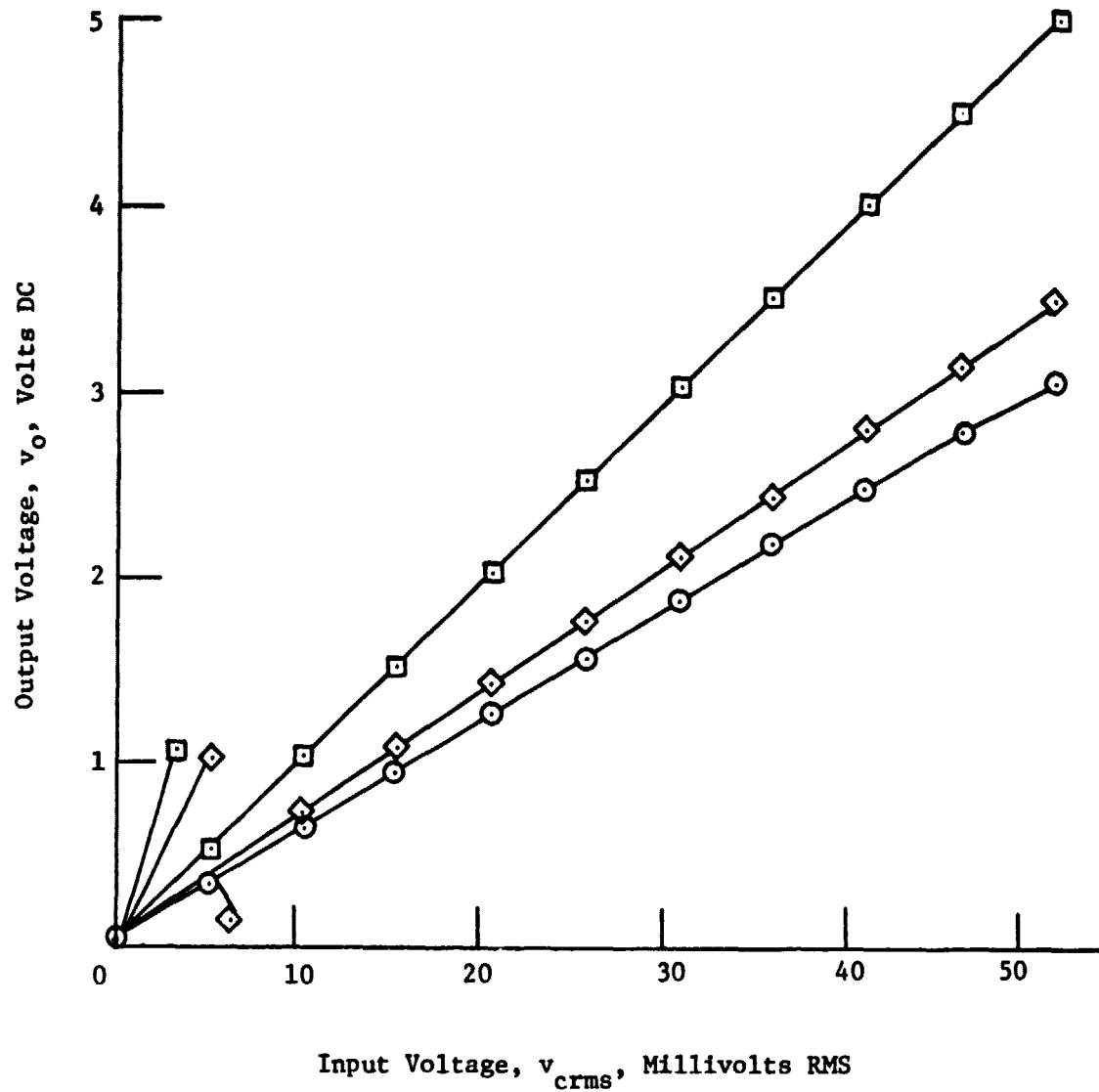


FIG. 12 - OUTPUT VOLTAGE VS. INPUT VOLTAGE FOR 5.0V DC BIAS VOLTAGE

Input Voltage Frequency: 12 Hz

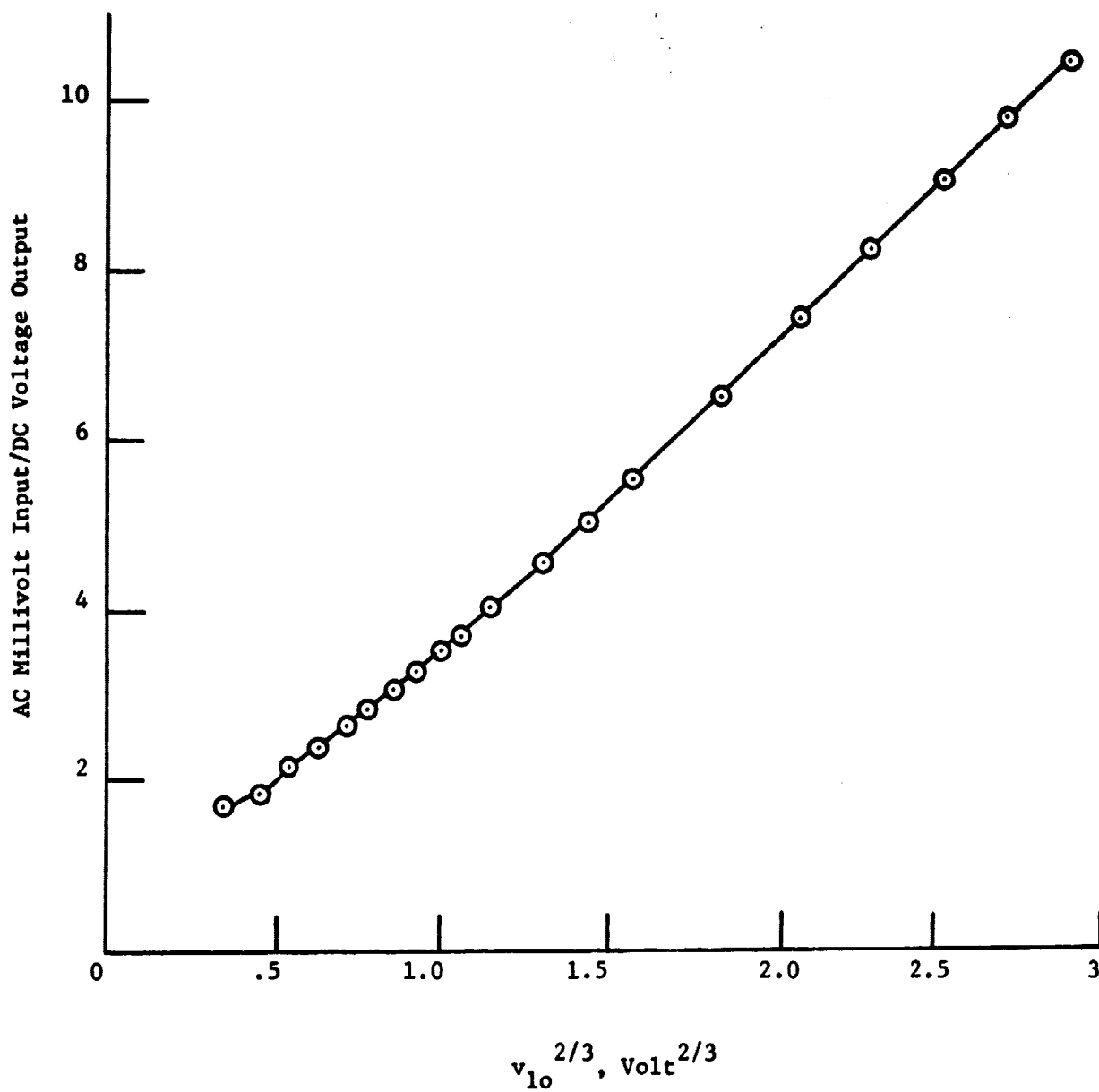
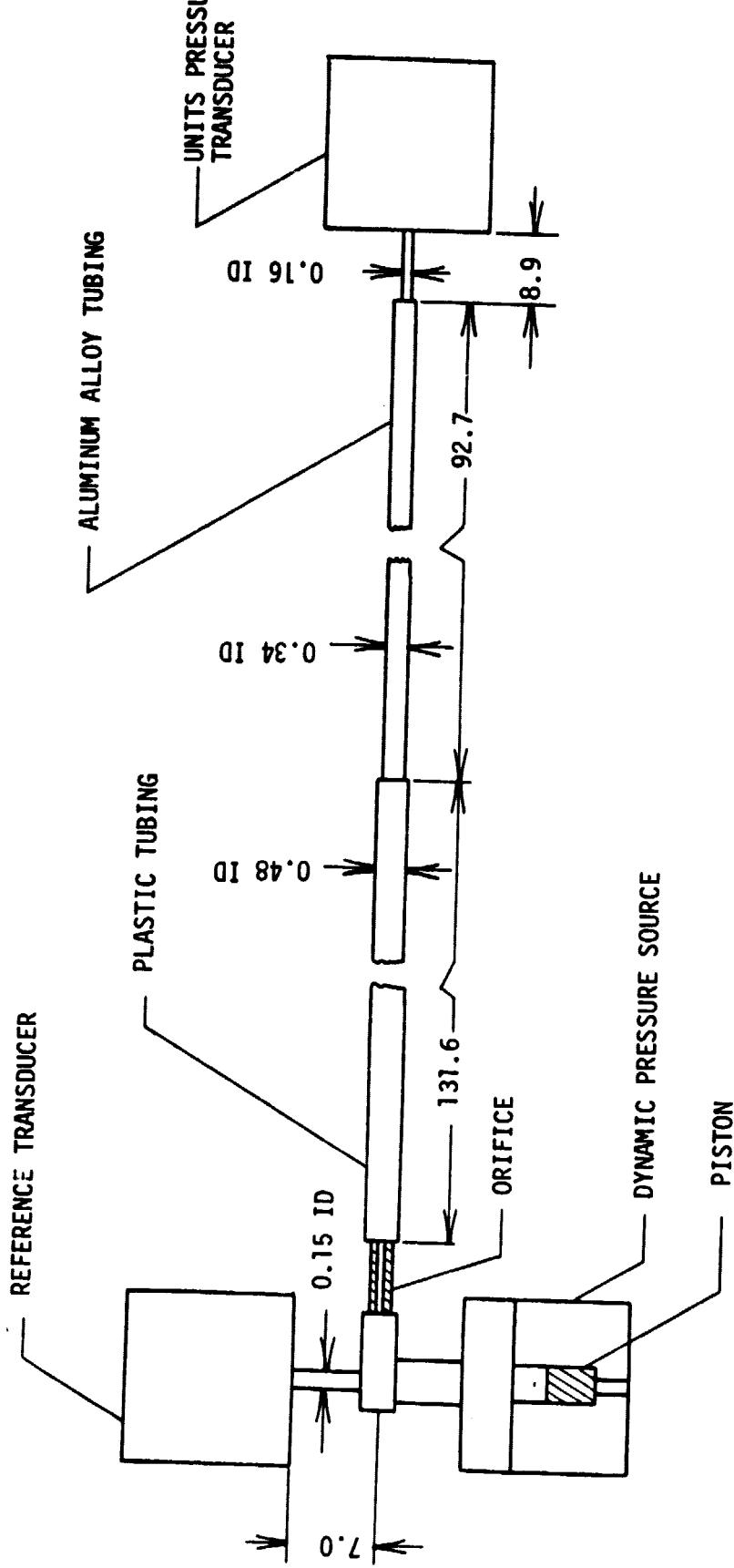


FIG. 13. AC INPUT VOLTAGE/DC OUTPUT VOLTAGE VS. DC INPUT VOLTAGE TO 2/3 POWER



All Dimensions in Centimeters

FIG. 14 - MOCK-UP OF TUBING CONFIGURATION USED UNITS APPLICATION

- #62 Orifice, 1.19 cm Length
- #65 Orifice, 1.27 cm Length
- ◇ #67 Orifice, 1.27 cm Length
- △ #68 Orifice, 1.27 cm Length
- ▴ #70 Orifice, 1.27 cm Length

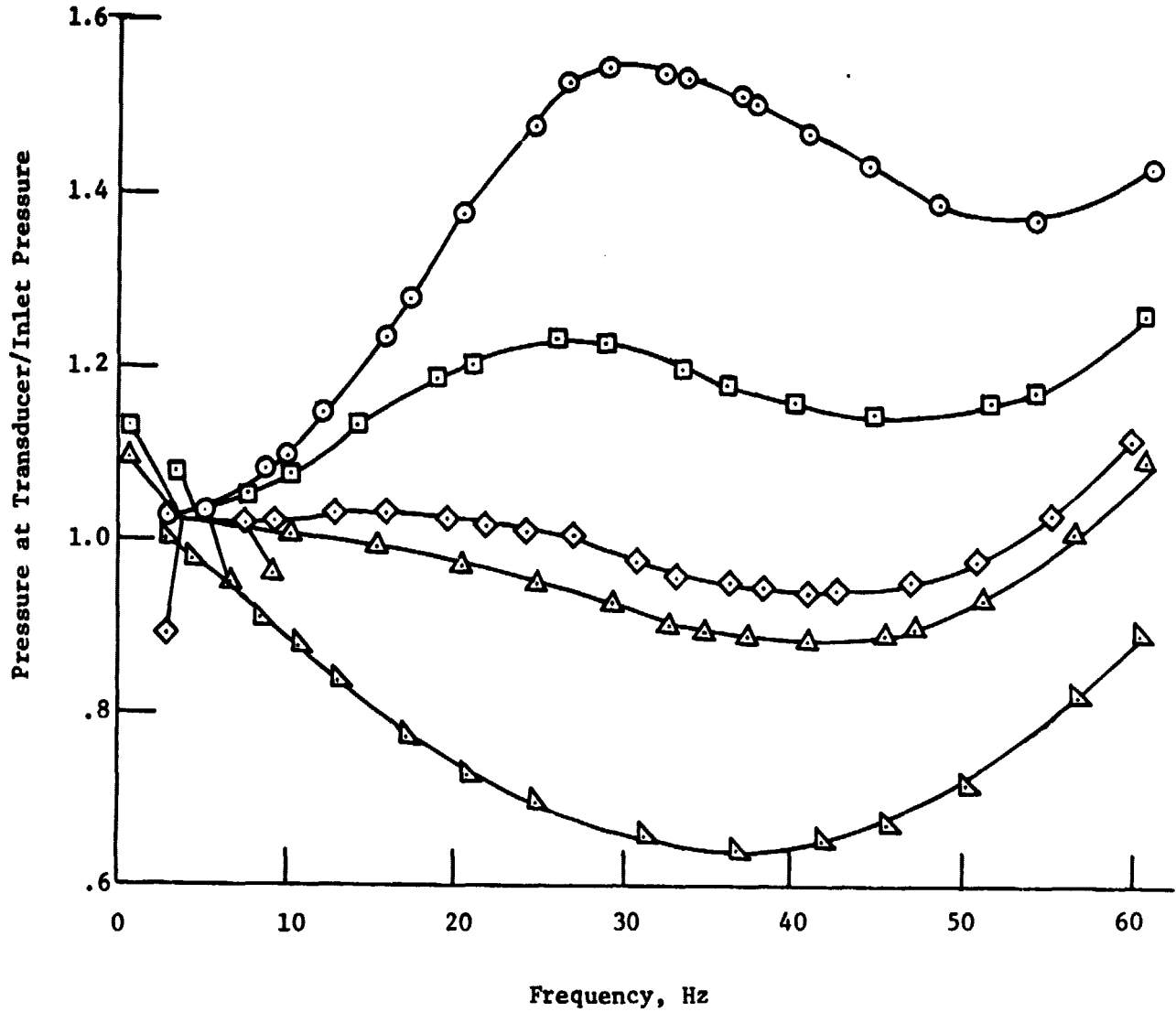


FIG. 15 - DYNAMIC RESPONSE CHARACTERISTIC OF TUBING MOCK-UP FOR VARIOUS ORIFICES